Available online at www.sciencedirect.com
ScienceDirect
Journal of Sound and Vibration 305 (2007) 904–917
JOURNAL OF SOUND AND VIBRATION
www.elsevier.com/locate/jsvi

Short Communication

Parametric instability of a cantilever beam with magnetic field and periodic axial load

Barun Pratiher, Santosha Kumar Dwivedy*

Indian Institute of Technology Guwahati, Guwahati 781039, India

Received 31 December 2006; received in revised form 18 April 2007; accepted 21 April 2007
Available online 15 June 2007

Abstract

The present work deals with the parametric instability regions of a cantilever beam with tip mass subjected to time-varying magnetic field and axial force. The nonlinear temporal differential equation of motion having two frequency parametric excitations is solved using second-order method of multiple scales. The closed-form expressions for the parametric instability regions for three different resonance conditions are determined. The influence of magnetic filed, axial load, damping constant and mass ratio on the parametric instability regions are investigated. These results obtained from perturbation analysis are verified by solving the temporal equation of motion using fourth-order Runge–Kutta method. The instability regions obtained using this method is found to be in good agreement with the experimental result.

1. Introduction

In the present work, a cantilever beam subjected to both periodic axial load and magnetic field is considered. This study will be used in the active vibration control of many structures such as flexible manipulators, foundations of rotating machinery, etc. These systems behave as parametrically excited systems and it is very important to determine the instability regions to avoid excessive vibrations due to resonance.

Here a few literatures related to the dynamic analysis of beams subjected to both the magnetic field and external forces are cited. Moon and Pao [1] investigated theoretically and experimentally the regions of instability of cantilever beam plate in a transverse magnetic field. Kojima and Nagana [2] studied the nonlinear vibration of a cantilever beam with tip mass subjected to alternating electromagnetic forces acting on the tip mass. Lu et al. [3] studied the dynamic stability and bifurcation of a simply supported beam subjected to magnetic field and alternating load by using method of multiples scales (MMS). Wu et al. [4] studied the dynamic stability of a cantilever beam with magnetic and axial force field using IHB method. Shih et al. [5] analyzed the transient vibrations of a simply supported beam subjected to both axial load and transverse magnetic field. Chen and Yah [6] investigated experimentally and analytically the parametric instability of a beam under electromagnetic excitation. Wu [7] investigated the instability regions of a simply supported beam subjected to magnetic field and thermal loading using IHB method. Recently, free vibration analysis of a

*Corresponding author.
E-mail address: dwivedy@iitg.ernet.in (S.K. Dwivedy).

0022-460X/$ - see front matter © 2007 Elsevier Ltd. All rights reserved.
doi:10.1016/j.jsv.2007.04.039

simply supported (S–S) and clamped–clamped (C–C) beam under magnetic field, axial and transverse loading is carried out by Liu and Chang [8].

Many researchers investigated the parametric instability regions of the cantilever beam subjected to time-varying axial load without considering the magnetic field. Burney and Jaeger [9] investigated the region of instability of a column hinged at both ends and subjected to periodic axial compressive load. Kar and Sujata [10] studied the parametric instability region of a cantilever beam subjected to a time-dependent axial force. Chen and Yah [11] studied the dynamic instability of a column carrying a concentrated mass with oscillating motion along the column axis. Hyun and Yoo [12] investigated the instability regions of a cantilever beam subjected to axial excitation using MMS. Chung et al. [13] investigated the instability regions of cantilever beam with rotary oscillation. In most of the cases, the system is reduced to that of a parametrically excited system with single frequency excitation. One may find different methods to determine the parametric instability regions in the books by Nayfeh and Mook [14], and Nayfeh and Balachandran [15].

It is observed that no studies have been carried out to find the instability regions of a cantilever beam with tip mass subjected to time-varying axial loading and magnetic field. Therefore, in the present work, an attempt has been made to study the dynamic instability of a cantilever beam with and without tip mass subjected to these loadings. In this work, the equation of motion is obtained by using extended Hamilton's principle, which is reduced to a damped Hill equation, by using generalized Galerkin's Method. This equation is similar to that of Wu et al. [4] where the system is considered to be a cantilever beam without any tip mass. They have used IHB method, which does not yield any closed-form solution. But in the present work second-order method of multiple scales is used to derive the analytical expressions for the regions of instability for three different resonance conditions. Effect of the magnetic filed, damping factor, axial force and mass ratio on instability regions are determined. The instability regions are verified by solving the temporal equation of motion. The instability region for a cantilever beam subjected to magnetic field is compared with the experimental result of Moon and Pao [1] and the numerical result of Wu et al. [4] and is found to be in good agreement.

2. The governing equation of motion of the systems

Figs. 1(a) and (b) show cantilever beams with and without tip mass subjected to time-dependent axial load $P = P_0 + P_1 \cos \Omega_1 t$ and transverse magnetic field $B_0 = B_m \cos \Omega_2 t$ where P_0, P_1, B_m, Ω_1 and Ω_2 are static axial force, amplitude of periodic axial force, strength of induced magnetic field, frequency of the periodic axial force and frequency of the magnetic field, respectively. Here L, d and h are the length, width and depth of the cantilever beam, respectively. The governing equation of motion of the cantilever beam is derived by using extended Hamilton's principle, which can be given by

$$m\ddot{Y} + C_d\dot{Y} + EIY'''' + (P_0 + P_1 \cos \Omega_1 t)Y'' - B_0^2 hd\left[\frac{\chi_m}{\mu_0\mu_r}Y'' + \sigma\left(Y''\int_0^x\int_0^\xi Y'(\eta)\dot{Y}'(\eta)\,d\eta\,d\xi + Y'\int_0^x Y'(\xi)\dot{Y}'(\xi)\,d\xi\right)\right] = 0. \quad (1)$$

This equation is similar to that obtained by Wu et al. [4] and Liu and Chang [8] but the boundary conditions are different. It may be noted that Liu and Chang [8] considered simply supported and clamped–clamped beam in their analysis.

Here, E and I are the Young modulus, moment of inertia of the cantilever beam and C_d is damping constant, m is the mass of the beam per unit length, m_b is the mass of the beam, m_t is the attached mass at the

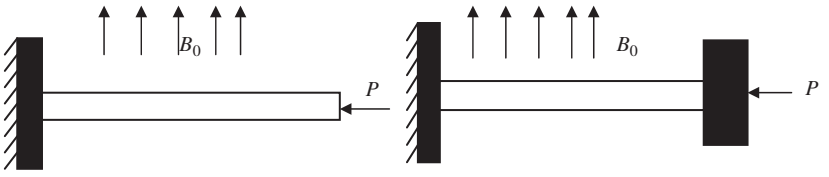

Fig. 1. Schematic diagram of the system (a) cantilever beam and (b) cantilever beam with tip mass subjected to both periodic axial load and magnetic field.

tip, μ_0 is the permeability of the vacuum, μ_r is the relative permeability, σ is the conductivity of the material and χ_m is the magnetic susceptibility. ξ, η are used as integration variables.

Now, the generalized Galerkin's Method is used to discretize the equation of motion (1) by using the following assumed mode shape:

$$Y(x,t) = r\psi(x)u(t), \tag{2}$$

where r is the scaling factor, $u(t)$ is the time modulation and $\psi(x)$ is the eigenfunction of the following system.

For system 1(a), $\psi(x)$ is the eigenfunction obtained from the free vibration of a cantilever beam which can be given by

$$\psi(x) = (\sin\,\beta L + \sinh\,\beta L)(\cos\,\beta x - \cosh\,\beta x) - (\cos\,\beta L + \cosh\,\beta L)(\sin\,\beta x - \sinh\,\beta x). \tag{3}$$

One may determine βL from the following equation:

$$1 + \cos\,\beta L\,\cosh\,\beta L = 0. \tag{4}$$

For system 1(b) $\psi(x)$ is the eigenfunction of a cantilever beam with tip mass, which can be given by

$$\psi(x) = -\left(\frac{\sin\,\beta L + \sinh\,\beta L}{\cos\,\beta L + \cosh\,\beta L}\right)(\cos\,\beta x - \cosh\,\beta x) + (\sin\,\beta x - \sinh\,\beta x). \tag{5}$$

In this case one may determine βL from the following equation:

$$\left[\cos\,\beta L + \cosh\,\beta L + \frac{m_t}{m_b}\beta L(\sin\,\beta L - \sinh\,\beta L)\right](\cos\,\beta L + \cosh\,\beta L) + \left[\sin\,\beta L - \sinh\,\beta L - \frac{m_t}{m_b}\beta L(\cos\,\beta L - \cosh\,\beta L)\right](\sin\,\beta L + \sinh\,\beta L) = 0. \tag{6}$$

The following nondimensional parameters are used in this analysis:

$$\bar{x} = \frac{x}{L}, \quad \tau = \omega_s t, \quad \bar{m} = \frac{m_t}{m_b}, \quad \bar{r} = \frac{r}{L}, \quad \bar{\Omega}_1 = \frac{\Omega_1}{\omega_s} \quad \text{and} \quad \bar{\Omega}_2 = \frac{\Omega_2}{\omega_s}.$$

By substituting Eq. (2) into Eq. (1) and using the above nondimensional terms, the resulting temporal differential equation of motion can be expressed as

$$\ddot{u} + 2\varepsilon\zeta\dot{u} + u + \varepsilon(\alpha_1\,\cos\,\bar{\Omega}_1\tau - \alpha_2\,\cos\,2\bar{\Omega}_2\tau)u - \varepsilon(\alpha_3 + \alpha_4)(1 + \cos\,2\bar{\Omega}_2\tau)u^2\dot{u} = 0. \tag{7}$$

Here ε is the book-keeping parameter. The expressions for the terms of linear frequency of the beam ω_L, system fundamental frequency ω_s, nondimensional amplitude of external axial force α_1, amplitude of magnetic force α_2 and amplitude of nonlinear inertia terms α_3, α_4 are given below:

$$\omega_L = \sqrt{\frac{EI}{mL^4}\frac{\int_0^1 \psi''''(\bar{x})\psi(\bar{x})\,\mathrm{d}\bar{x}}{\int_0^1(\psi(\bar{x}))^2\,\mathrm{d}\bar{x}}},$$

$$\omega_s = \sqrt{\frac{EI}{mL^4}\frac{\int_0^1 \psi''''(\bar{x})\psi(\bar{x})\,\mathrm{d}\bar{x}}{\int_0^1(\psi(\bar{x}))^2\,\mathrm{d}\bar{x}} + \frac{P_0}{mL^2}\frac{\int_0^1 \psi''(\bar{x})\psi(\bar{x})\,\mathrm{d}\bar{x}}{\int_0^1(\psi(\bar{x}))^2\,\mathrm{d}\bar{x}} - \frac{\chi_m B_m^2 hd}{2\mu_0\mu_r mL^2}\frac{\int_0^1 \psi''(\bar{x})\psi(\bar{x})\,\mathrm{d}\bar{x}}{\int_0^1(\psi(\bar{x}))^2\,\mathrm{d}\bar{x}}},$$

$$\alpha_1 = \frac{P_1}{\varepsilon m\omega_s^2 L^2}\frac{\int_0^1 \psi''(\bar{x})\psi(\bar{x})\,\mathrm{d}\bar{x}}{\int_0^1(\psi(\bar{x}))^2\,\mathrm{d}\bar{x}}, \quad \alpha_2 = \frac{\chi_m B_m^2 hd}{2\varepsilon\mu_0\mu_r mL^2\omega_s^2}\frac{\int_0^1 \psi''(\bar{x})\psi(\bar{x})\,\mathrm{d}\bar{x}}{\int_0^1(\psi(\bar{x}))^2\,\mathrm{d}\bar{x}}, \quad B_r^2 = \frac{B_m^2}{2},$$

$$\frac{1}{B_c^2} = \frac{\chi hd}{\mu_0\mu_r mL^2\omega_s^2}\frac{\int_0^1 \psi''(\bar{x})\psi(\bar{x})\,\mathrm{d}\bar{x}}{\int_0^1(\psi(\bar{x}))^2\,\mathrm{d}\bar{x}}, \quad \alpha_3 = \frac{\sigma hd B_m^2\bar{r}^2}{2\varepsilon m\omega_s}\frac{\int_0^1 \psi''(\bar{x})\psi(\bar{x})\int_0^{\bar{\eta}}\int_0^{\bar{\xi}}\psi'(\bar{x})\psi'(\bar{x})\mathrm{d}\bar{\eta}\,\mathrm{d}\bar{\xi}\,\mathrm{d}\bar{x}}{\int_0^1(\psi(\bar{x}))^2\,\mathrm{d}\bar{x}},$$

$$\alpha_4 = \frac{\sigma hd B_m^2\bar{r}^2}{2\varepsilon m\omega_s}\frac{\int_0^1 \psi'(\bar{x})\psi(\bar{x})\int_0^{\bar{\xi}}\psi'(\bar{x})\psi'(\bar{x})\mathrm{d}\bar{\xi}\,\mathrm{d}\bar{x}}{\int_0^1(\psi(\bar{x}))^2\,\mathrm{d}\bar{x}}. \tag{8}$$

Eq. (7) is similar to that of temporal Eq. (18) of Liu and Chang [8] neglecting the external force (f) and stiffness term (k) and [4]. But, it may be noted that Liu and Chang [8] studied only the free vibration by solving the

temporal equation numerically using fourth-order Runge–Kutta method for S–S and C–C beams. Wu et al. [4] studied instability regions and vibration motion of cantilever beam without considering the tip mass and they used IHB method for finding the instability regions which does not yield any closed-form solution. To study the parametric instability regions of the trivial state, one may reduce the temporal equation of motion (7) to the following linear damped Hill's equation:

$$\ddot{u} + 2\varepsilon\mu\dot{u} + u + \varepsilon(\alpha_1 \cos \bar{\Omega}_1\tau - \alpha_2 \cos 2\bar{\Omega}_2\tau)u = 0. \tag{9}$$

The analytical expressions for the parametric instability regions are determined by using the second-order method of multiple scales as described in the following section.

3. The perturbation analysis

Here, the method of multiple scales is used to find the analytical expressions for the instability regions. In this method, displacement u can be represented in terms of different times scale (T_0, T_1, T_2) and a book-keeping parameter ε as follows:

$$u(\tau;\varepsilon) = u_0(T_0, T_1, T_2) + \varepsilon u_1(T_0, T_1, T_2) + \varepsilon^2 u_2(T_0, T_1, T_2) + O(\varepsilon^3), \tag{10}$$

here $T_0 = \tau$, $T_1 = \varepsilon\tau$ and $T_2 = \varepsilon^2\tau$. The transformations of first and second time derivatives are given by

$$\frac{\mathrm{d}}{\mathrm{d}\tau} = D_0 + \varepsilon D_1 + \varepsilon^2 D_2 + O(\varepsilon^2), \tag{11}$$

$$\frac{d^2}{\mathrm{d}\tau^2} = D_0^2 + 2\varepsilon D_0 D_1 + \varepsilon^2(D_1^2 + 2D_0 D_2) + O(\varepsilon^3), \tag{12}$$

where $D_0 = \partial/\partial T_0$, $D_1 = \partial/\partial T_1$ and $D_2 = \partial/\partial T_2$. Substituting Eqs. (10), (11) and (12) into Eq. (9) and equating the coefficient of like powers of ε, yields the following equations:

$$\text{Order } \varepsilon^0: \quad D_0^2 u_0 + u_0 = 0, \tag{13}$$

$$\text{Order } \varepsilon^1: \quad D_0^2 u_1 + u_1 = -2D_0 D_1 u_0 - 2\mu D_0 u_0 - \alpha_1 \cos(\bar{\Omega}_1\tau)u_0 + \alpha_2 \cos(2\bar{\Omega}_2\tau)u_0, \tag{14}$$

$$\begin{aligned}\text{Order } \varepsilon^2: \quad D_0^2 u_2 + u_2 = {} & -2D_0 D_1 u_1 - 2\mu D_1 u_0 - 2\mu D_0 u_1 - (D_1^2 + 2D_0 D_2)u_0 \\ & - \alpha_1 \cos(\bar{\Omega}_1\tau)u_1 + \alpha_2 \cos(2\bar{\Omega}_2\tau)u_1.\end{aligned} \tag{15}$$

General solutions of Eq. (13) can be written as

$$u_0 = A(T_1, T_2)\exp(\mathrm{i}T_0) + \bar{A}(T, T_2)\exp(-\mathrm{i}T_0). \tag{16}$$

Substituting Eq. (16) into Eq. (14) leads to

$$\begin{aligned}D_0^2 u_1 + u_1 = {} & -2\mathrm{i}A' \exp(\mathrm{i}T_0) - 2\mathrm{i}\mu A \exp(\mathrm{i}T_0) - \frac{\alpha_1}{2}[A \exp \mathrm{i}(1 + \bar{\Omega}_1)T_0 + \bar{A} \exp \mathrm{i}(\bar{\Omega}_1 - 1)T_0] \\ & + \frac{\alpha_2}{2}[A \exp \mathrm{i}(1 + 2\bar{\Omega}_2)T_0 + \bar{A} \exp \mathrm{i}(2\bar{\Omega}_2 - 1)T_0] + \text{cc}.\end{aligned} \tag{17}$$

One may observe that any solution of Eq. (17) will contain secular or small divisor terms when nondimensional frequency of external axial loading ($\bar{\Omega}_2$) is nearly equal to 2 and/or nondimensional frequency of magnetic field ($\bar{\Omega}_2$) is nearly equal to 1. Hence, one may have three different resonance conditions viz. (i) ($\bar{\Omega}_1$) ≈ 2 and $\bar{\Omega}_2$ is away from 1, (ii) $\bar{\Omega}_2 \approx 1$ and $\bar{\Omega}_1$ is away from 2 and (iii) $\bar{\Omega}_2 \approx 2$ and $\bar{\Omega}_1 \approx 1$ simultaneously. These three conditions are discussed in the following sections.

3.1. Case 1: $\bar{\Omega}_1 \approx 2$ and $\bar{\Omega}_2$ is away from 1

For this case, to express the nearness of $\bar{\Omega}_1$ to 2, one may use the detuning parameter σ as

$$\bar{\Omega}_1 = 2 + 2\varepsilon\sigma, \quad \sigma = O(1). \tag{18}$$

Substituting Eq. (18) into Eq. (17) and eliminating the secular or small divisor terms yields

$$2\mathrm{i}A' + 2\mathrm{i}\mu A + \frac{\alpha_1}{2}\bar{A}\ \exp\ \mathrm{i}(2\sigma T_1) = 0. \tag{19}$$

One may write the particular solution of Eq. (17) as

$$u_1 = \frac{\alpha_1}{2[(1+\bar{\Omega}_1)^2 - 1]}(A(T_1)\exp\ \mathrm{i}(1+\bar{\Omega}_1)\tau) - \frac{\alpha_2}{2[(1+2\bar{\Omega}_2)^2 - 1]}(A(T_1)\exp\ \mathrm{i}(1+2\bar{\Omega}_2)\tau) - \frac{\alpha_2}{2[(1-2\bar{\Omega}_2)^2 - 1]}(A(T_1)\exp\ \mathrm{i}(2\bar{\Omega}_2 - 1)\tau) + \mathrm{cc}. \tag{20}$$

Substituting Eqs. (16) and (20) into Eq. (15) and eliminating the secular or small divisor terms yields

$$2\mathrm{i}D_2A + 2\mu D_1A + D_1^2A + \Gamma A = 0, \tag{21}$$

where

$$\Gamma = \frac{1}{2}\left(\frac{\alpha_1^2}{4\bar{\Omega}_1 + 2\bar{\Omega}_1^2}\right) + \frac{1}{2}\left(\frac{\alpha_2^2}{8\bar{\Omega}_2 + 8\bar{\Omega}_2^2}\right) + \frac{1}{2}\left(\frac{\alpha_2^2}{-8\bar{\Omega}_2 + 8\bar{\Omega}_2^2}\right).$$

From Eq. (19), one may obtain

$$D_1^2A = \mu^2A + \left(\frac{\alpha_1}{4}\right)^2A - \frac{\alpha_1}{4}(2\mu\mathrm{i} + 2\sigma)\bar{A}\ \exp(2\mathrm{i}\sigma T_1). \tag{22}$$

Substituting Eqs. (19) and (22) into Eq. (21) gives

$$2\mathrm{i}D_2A + \left(-\mu^2 + \left(\frac{\alpha_1}{4}\right)^2 + \Gamma\right)A - \frac{\alpha_1}{2}\sigma\bar{A}\ \exp(2\mathrm{i}\sigma T_1) = 0. \tag{23}$$

Substituting Eqs. (19) and (23) to Eq. (11), one may obtain the following equation:

$$2\mathrm{i}\,\frac{\mathrm{d}A}{\mathrm{d}\tau} + \left(2\mathrm{i}\varepsilon\mu + \varepsilon^2\left[-\mu^2 + \left(\frac{\alpha_1}{4}\right)^2 + \Gamma\right]\right)A + \frac{\alpha_1}{4}(\varepsilon - 2\varepsilon^2\sigma)\bar{A}\ \exp(2\mathrm{i}\sigma T_1) = 0. \tag{24}$$

Putting $A = (B_r + \mathrm{i}B_i)\exp(\mathrm{i}\varepsilon\sigma\tau)$, where B_r and B_i are real and imaginary parts in Eq. (24) and separating the real and imaginary parts yield the following equations:

$$2\frac{\mathrm{d}B_r}{\mathrm{d}\tau} + 2\varepsilon\mu B_r + \left[2\varepsilon\sigma + \varepsilon\frac{\alpha_1}{2} - \varepsilon^2\left(\frac{\alpha_1}{2}\sigma\right) - \left(-\mu^2 + \left(\frac{\alpha_1}{4}\right)^2 + \Gamma\right)\right]B_i = 0, \tag{25}$$

$$2\frac{\mathrm{d}B_i}{\mathrm{d}\tau} + 2\varepsilon\mu B_i + \left[-2\varepsilon\sigma + \varepsilon\frac{\alpha_1}{2} - \varepsilon^2\left(-\frac{\alpha_1}{2}\sigma\right) + \left(-\mu^2 + \left(\frac{\alpha_1}{4}\right)^2 + \Gamma\right)\right]B_r = 0. \tag{26}$$

Substituting $(B_r,\ B_i) = (b_r, b_i)\exp(\gamma\tau)$ into Eqs. (25) and (26) yields the following equations:

$$2\gamma b_r + 2\varepsilon\mu b_r + \left[2\varepsilon\sigma + \varepsilon\frac{\alpha_1}{2} - \varepsilon^2\left(\frac{\alpha_1}{2}\sigma\right) - \left(-\mu^2 + \left(\frac{\alpha_1}{4}\right)^2 + \Gamma\right)\right]b_i = 0, \tag{27}$$

$$2\gamma b_i + 2\varepsilon\mu b_i + \left[-2\varepsilon\sigma + \varepsilon\frac{\alpha_1}{2} - \varepsilon^2\left(-\frac{\alpha_1}{2}\sigma\right) + \left(-\mu^2 + \left(\frac{\alpha_1}{4}\right)^2 + \Gamma\right)\right]b_r = 0. \tag{28}$$

For steady-state trivial response, γ is equal to zero. One may obtain the expression for the transition curves by finding the value of σ from the above two equations. Neglecting the terms $O(\varepsilon^3)$, one may write the expression for transition curves of the second-order expansion when $\bar{\Omega}_1 \approx 2$ as

$$\bar{\Omega}_1 = 2 \pm \varepsilon\sqrt{\left(\varepsilon^2\left(\mu^2 + 3\left(\frac{\alpha_1}{4}\right)^2 - \Gamma\right)^2 + 4\left(\frac{\alpha_1^2}{16} - \mu^2\right)\right)} - \varepsilon^2\left(\mu^2 + 3\left(\frac{\alpha_1}{4}\right)^2 - \Gamma\right). \tag{29}$$

3.2. Case 2: $\bar{\Omega}_2 \approx 1$ and $\bar{\Omega}_1$ is away from 2

Following the method similar to that described in Section 3.1, for this simple resonance case $\bar{\Omega}_2 \approx 1$ ($\bar{\Omega}_2 = 1 + \varepsilon\sigma$) and $\bar{\Omega}_1$ is away from 2, the transition curves emanating from $\bar{\Omega}_2 \approx 1$ may be written as

$$\bar{\Omega}_2 = 1 \pm \frac{\varepsilon}{2}\sqrt{\left(\varepsilon^2\left(\mu^2 + 3\left(\frac{\alpha_1}{4}\right)^2 - \Gamma\right)^2 + 4\left(\frac{\alpha_1^2}{16} - \mu^2\right)\right)} - \frac{\varepsilon^2}{2}\left(\mu^2 + 3\left(\frac{\alpha_1}{4}\right)^2 - \Gamma\right). \tag{30}$$

Here,

$$\Gamma = \frac{1}{2}\left(\frac{\alpha_1^2}{4\bar{\Omega}_1 + 2\bar{\Omega}_2^2}\right) + \frac{1}{2}\left(\frac{\alpha_1^2}{-4\bar{\Omega}_1 + 2\bar{\Omega}_1^2}\right) + \frac{1}{2}\left(\frac{\alpha_2^2}{8\bar{\Omega}_2 + 8\bar{\Omega}_2^2}\right).$$

3.3. Case 3: $\bar{\Omega}_1 \approx 2$ and $\bar{\Omega}_2 \approx 1$

In this resonance condition when the system is excited simultaneously by the external force and the magnetic field, the frequency of excitation can be given by $\Omega = \bar{\Omega}_1 = 2\bar{\Omega}_2 = 2 + 2\varepsilon\sigma$. Following the method similar to that described in Sections 3.1 and 3.2, the expression for the transition curves can be given by

$$\Omega = 2 \pm \varepsilon\sqrt{\left(\varepsilon^2\left(\mu^2 + 3\left(\frac{\alpha_1 - \alpha_2}{4}\right)^2 - \Gamma\right)^2 + 4\left(\frac{(\alpha_1 - \alpha_2)^2}{16} - \mu^2\right)\right)} - \varepsilon^2\left(\mu^2 + 3\left(\frac{\alpha_1 - \alpha_2}{4}\right)^2 - \Gamma\right). \tag{31}$$

Here,

$$\Gamma = -\frac{1}{2}\left(\frac{\alpha_1^2}{4\bar{\Omega}_1 + 2\bar{\Omega}_1^2}\right) + \frac{1}{2}\left(\frac{\alpha_1\alpha_2}{4\bar{\Omega}_1 + 2\bar{\Omega}_1^2}\right) - \frac{1}{2}\left(\frac{\alpha_2^2}{8\bar{\Omega}_2 + 8\bar{\Omega}_2^2}\right) + \frac{1}{2}\left(\frac{\alpha_1\alpha_2}{8\bar{\Omega}_1 + 8\bar{\Omega}_1^2}\right).$$

4. Numerical results and discussions

In all simulations, a steel beam with length $L = 0.5\,\text{m}$, width $d = 0.001\,\text{m}$, depth $h = 0.005\,\text{m}$, Young's Modulus $E = 1.94 \times 10^{11}\,\text{N/m}^2$, mass of the beam $m = 0.04\,\text{kg}$, the permeability of the vacuum, $\mu_0 = 1.26 \times 10^{-06}\,\text{H m}^{-1}$ and relative permeability $\mu_r = 3000$ are considered. In Section 4.1, the results for the case with nondimensional frequency of magnetic field $\bar{\Omega}_2 \approx 1$ and nondimensional frequency of external axial loading $\bar{\Omega}_1$ away from 2, in Section 4.2 the results for the case with $\bar{\Omega}_1 \approx 2$ and $\bar{\Omega}_2$ away from 1 and in Section 4.3 the results for the case with $\bar{\Omega}_1 \approx 2$ and $\bar{\Omega}_2 \approx 1$ are presented. The instability regions are plotted and the effect of the key parameters like magnetic field B_0, damping constant C_d, static axial force P_0, amplitude of axial periodic load P_1 and mass ratio $\bar{m}$ on the region of instability are investigated. In these plots, the regions bounded by the curves are unstable and regions outside the curves are stable.

4.1. Simple resonance due to magnetic field ($\bar{\Omega}_2 \approx 1$ and $\bar{\Omega}_1$ is away from 2)

In this case, the system is subjected to magnetic field with a frequency nearly equal to the natural frequency of the system and the frequency of external axial loading is away from the principal parametric instability zone. Fig. 2 shows the parametric instability region in $(\Omega_2/\omega_L)^2 \sim (B_r/B_c)^2$ plane for a cantilever beam subjected to only the transverse magnetic field. For comparison purpose, the instability region obtained experimentally and numerically by Moon and Pao (Wu et al. [4]) is also being plotted. It is observed that the present result and the experimental result of Moon and Pao [1] are in very good agreement. It may be noted that Wu et al. [4] also obtained similar result by a different method (i.e., IHB method). But they have not studied the case of cantilever beam with tip mass. Also, the IHB method does not yield any close-form expression as obtained in the present work.

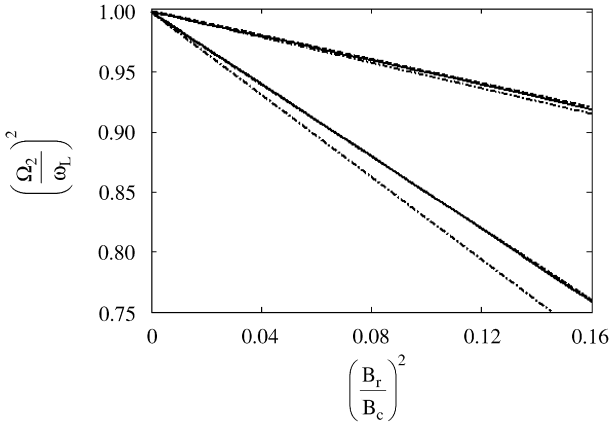

Fig. 2. Region of instability in magnetic field, - · - · - · -, Pao's theoretical result; - - - -, Pao's experimental result; and ——, present result.

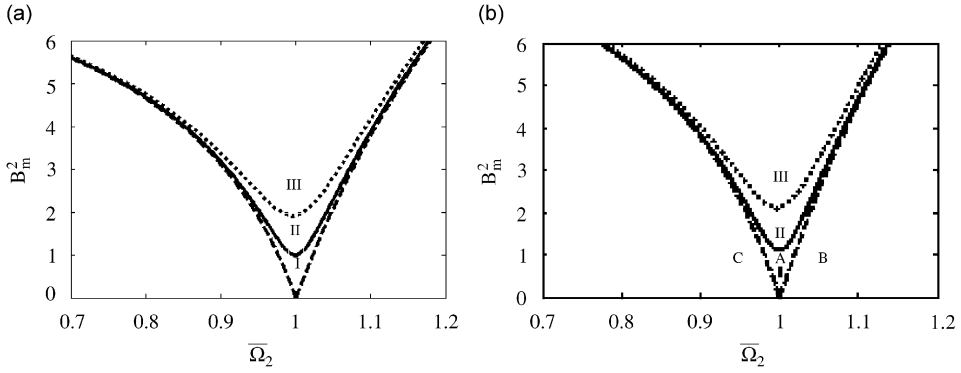

Fig. 3. Influence of the static axial force on the transition curves in magnetic field for cantilever beam without tip mass (I) $C_d = 0.0$, (II) $C_d = 0.2$ and (III) $C_d = 0.4$; (a) $P_0 = 5$ and (b) $P_0 = 10$.

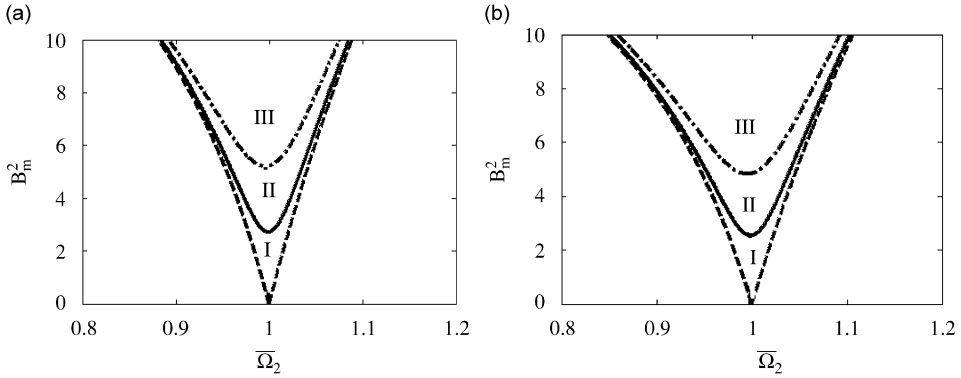

Fig. 4. Influence of the mass ratio on the transition curves in magnetic field for cantilever beam with tip mass for $P_0 = 1.0$; (I) $C_d = 0.0$, (II) $C_d = 0.2$ and (III) $C_d = 0.4$; (a) $\bar{m} = 0.1$ and (b) $\bar{m} = 0.2$.

To thoroughly study the instability region for different system parameters, in the following figures, they are plotted either in $P_1 \sim \bar{\Omega}_1$ or in $B_m^2 \sim \bar{\Omega}_2$ plane. Figs. 3 and 4 respectively show the influence of static load parameter P_0 and mass ratio $\bar{m}$ on the instability regions.

From Fig. 3, one may observe that with increase in static force the parametric instability region is decreased. One may note from Figs. 3 and 4 that with decrease in mass ratio $\bar{m}$ and with increase in damping C_d the region of instability get decreased. It may be observed that these instability regions are independent of P_1 as the frequency of axial loading is away from the principal parametric zone.

The instability regions obtained in this resonance case are verified by solving the temporal differential equation (7). The time responses for three points in the instability regions are determined (points of A, B and C of Figs. 3(b and I)) with damping $C_d = 0.0$ as shown in Figs. 5(a–c). It may clearly be observed from the time responses that while points B and C are stable trivial-state response, point A is unstable, which is in good agreement with the perturbation analysis.

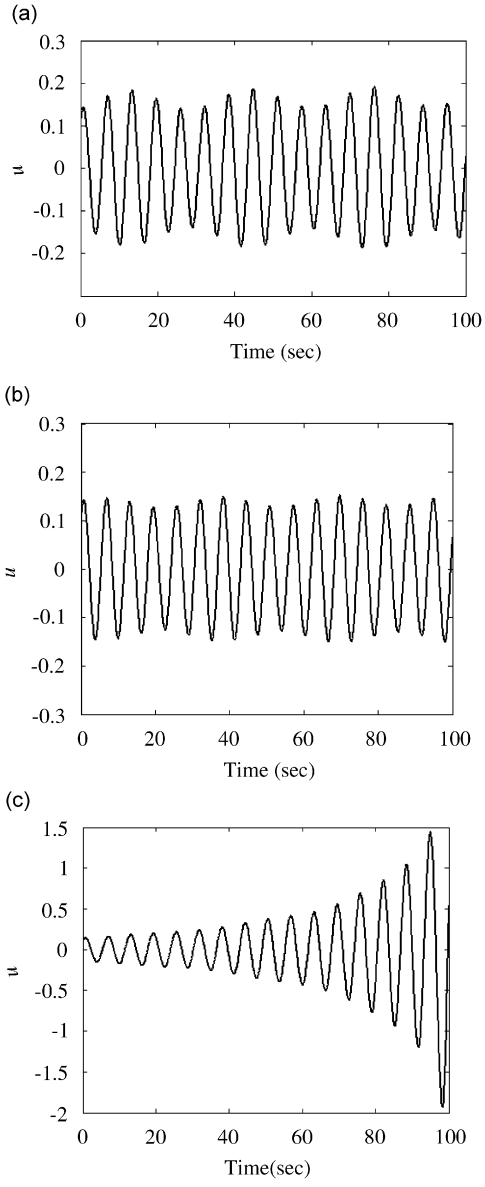

Fig. 5. Time response for (a) point C; (b) point B and (c) point A; key as in Fig. 3(b, I).

4.2. Principal parametric resonance due to external loading ($\bar{\Omega}_1 \approx 2$, $\bar{\Omega}_2$ away from 1)

In this section, effects of damping constant, magnetic field, static axial force and mass ratio on the parametric instability regions in periodic axial force field are investigated. Figs. 6–8 show the instability

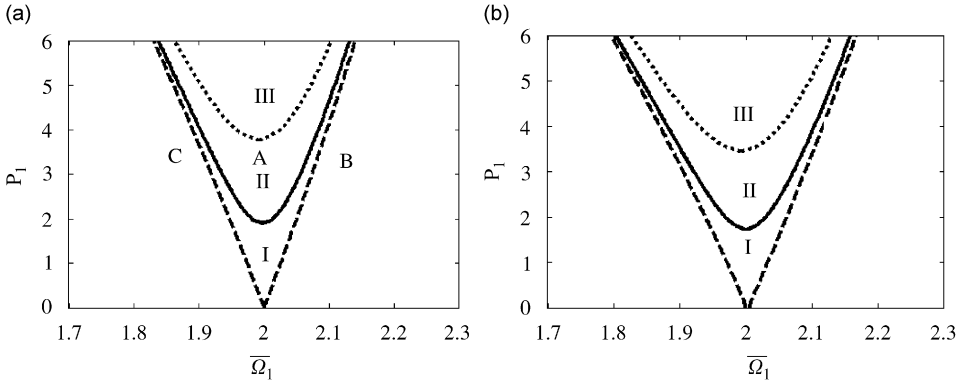

Fig. 6. Influence of the magnetic filed on the transition curves in periodic axial force field for cantilever beam without tip mass for $P_0 = 1.0$; (I) $C_d = 0.0$, (II) $C_d = 0.2$ and (III) $C_d = 0.4$; (a) $B_m = 0.3$ and (b) $B_m = 1.3$.

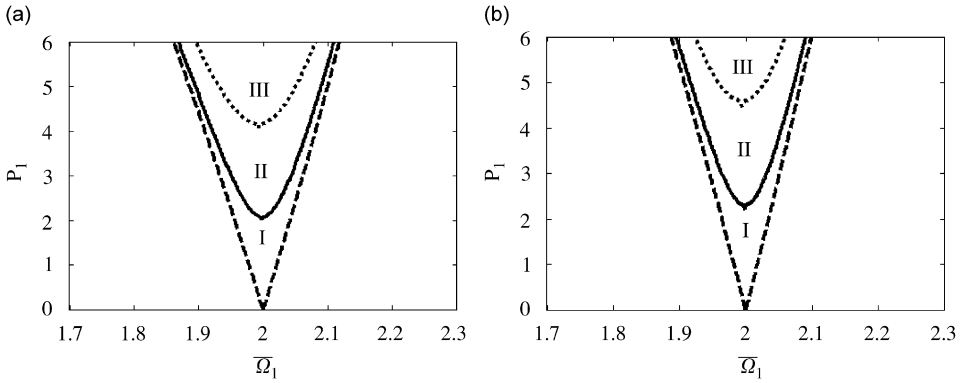

Fig. 7. Influence of the static axial force on the transition curves in periodic axial force field for cantilever beam without tip mass for $B_m = 0.3$; (I) $C_d = 0.0$, (II) $C_d = 0.2$ and (III) $C_d = 0.4$; (a) $P_0 = 5$ and (b) $P_0 = 10$.

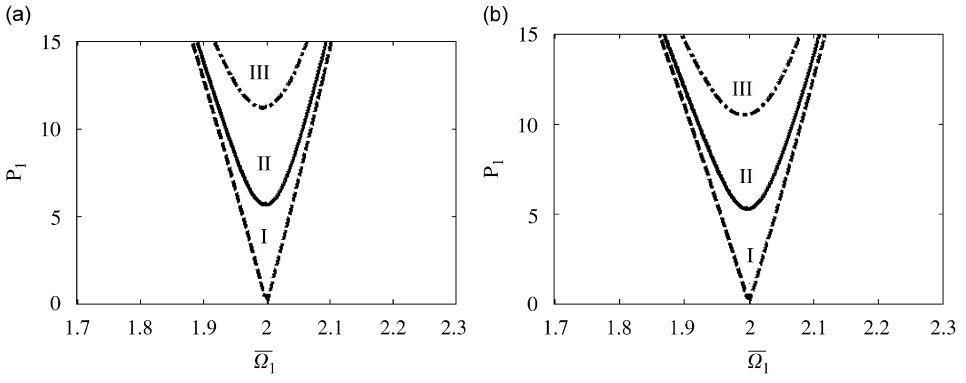

Fig. 8. Influence of the mass ratio on the transition curves in periodic axial force field for cantilever beam with tip mass for $B_m = 0.3$ and $P_0 = 1.0$, (I) $C_d = 0.0$, (II) $C_d = 0.2$ and (III) $C_d = 0.4$; (a) $\bar{m} = 0.1$ and (b) $\bar{m} = 0.2$.

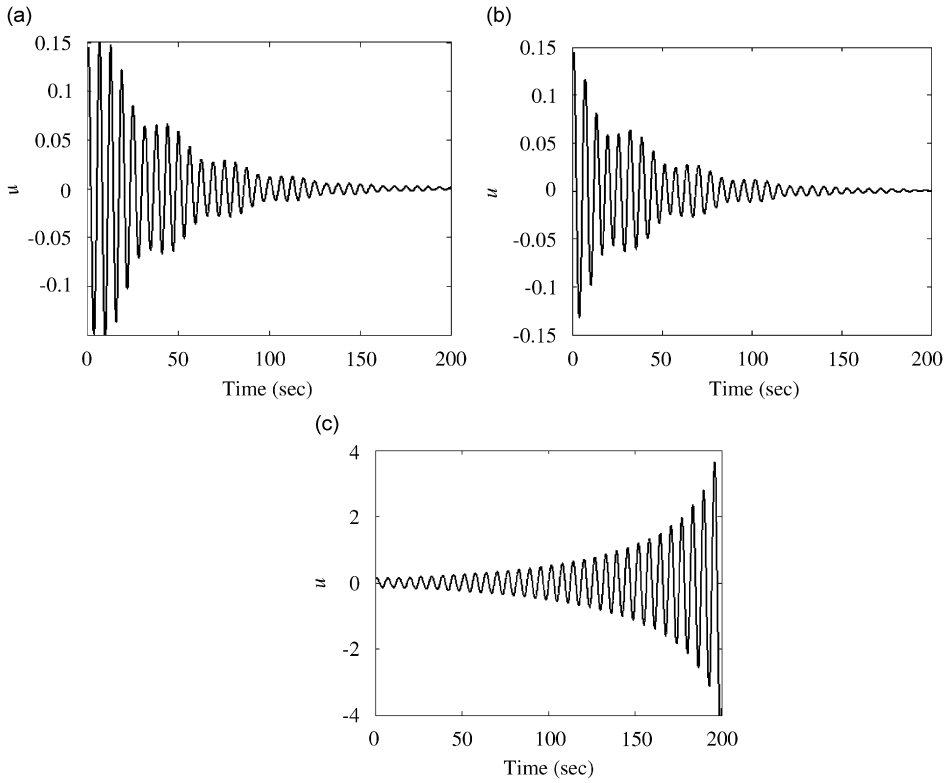

Fig. 9. Time response for (a) point C; (b) point B and (c) point A; key as in Fig. 6(a, II).

regions when the system is excited at a frequency $\bar{\Omega}_1 \simeq 2$ (i.e., nearly equal to twice the fundamental frequency) and $\bar{\Omega}_2$ is away from 1.

In Fig. 6, the influence of magnetic field and damping on the instability regions for the system shown in Fig. 1(a) are investigated. It is observed that with increase in magnetic field strength B_m, the instability region increases and with increase in damping the system becomes more stable. Fig. 7 shows the influence of static load parameter P_0 and damping on the parametric instability regions for the same system. From Figs. 6(a) and 7(a, b), it is apparent that with increase in P_0 the instability regions decrease. This is due to the fact that with increases in P_0 the natural frequency of the system increases, which reduces the range of instability regions. Fig. 8 shows the influence of mass ratio $\bar{m}$ (ratio of the tip mass to the mass of the beam) on the instability regions for the system shown in Fig. 1(b). As with increase in mass ratio, the natural frequency ω_L decreases, $\bar{\Omega}_1$ increases. This causes the increase in the instability region, which may be noted from Figs. 6–8. From all these figures, it is observed that damping improves the stability of the system.

Similar to the previous case, here also for the principal parametric resonance case, i.e., $\bar{\Omega}_1 \approx 2$, one may verify the instability regions obtained using the perturbation analysis by plotting the time response which are determined numerically by solving the temporal Eq. (7). Figs. 9(a–c) show the time responses for three points A, B and C which are marked in Fig. 6(a, II) with $C_d = 0.2$. In Fig. 6, it is shown that while points B and C are in stable region point A is in the unstable regions, which are in good agreement with the time response obtained from the temporal equation.

4.3. Simultaneous principal parametric and simple resonance ($\bar{\Omega}_1 \approx 2$ and $\bar{\Omega}_2 \approx 1$)

In this case, the system is subjected to magnetic field with a frequency nearly equal to the natural frequency of the system and an external axial loading with a frequency nearly equal to twice the fundamental frequency.

Hence the system is subjected to simultaneous principal parametric resonance due to external axial loading and simple resonance due to magnetic field.

In this case, Fig. 10 shows the influence of magnetic field and damping on the transition curves for the system shown in Fig. 1(a). It is observed that with increase in magnetic field and damping the stability of the

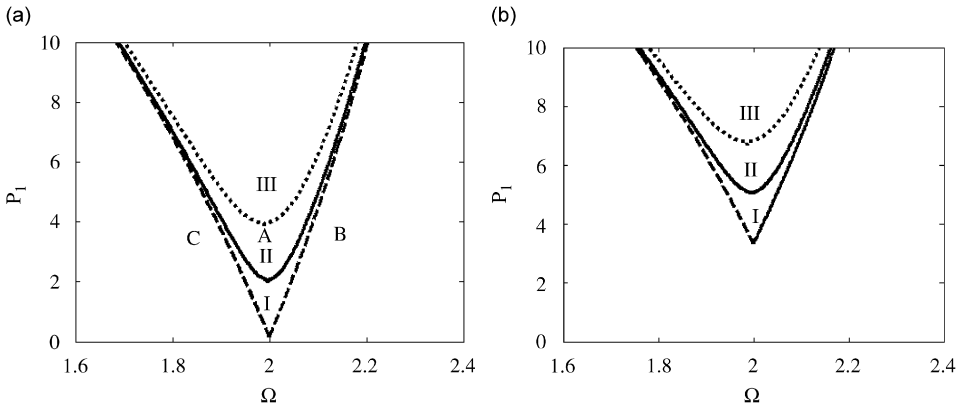

Fig. 10. Influence of the magnetic filed on the transition curves cantilever beam without tip mass for $P_0 = 1.0$, (I) $C_d = 0.0$, (II) $C_d = 0.2$ and (III) $C_d = 0.4$; (a) $B_m = 0.3$ and (b) $B_m = 1.3$.

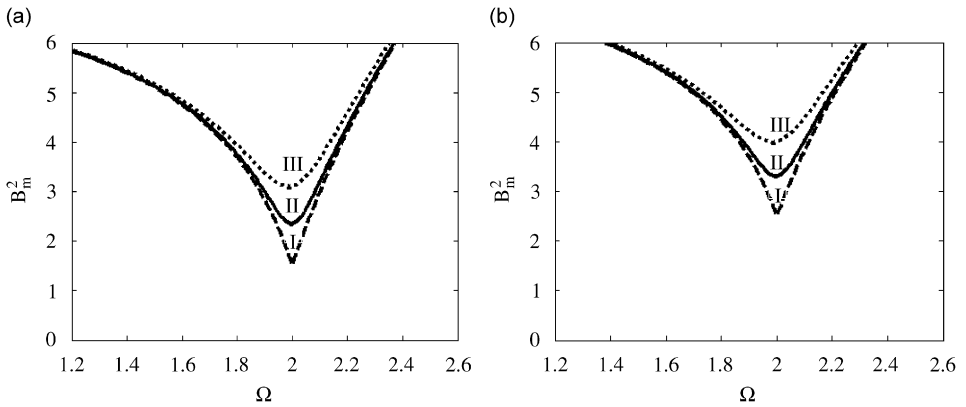

Fig. 11. Influence of the periodic axial force on the transition curves cantilever beam without tip mass for $P_1 = 1.0$, (I) $C_d = 0.0$, (II) $C_d = 0.2$ and (III) $C_d = 0.4$; (a) $P_0 = 3$ and (b) $P_0 = 5$.

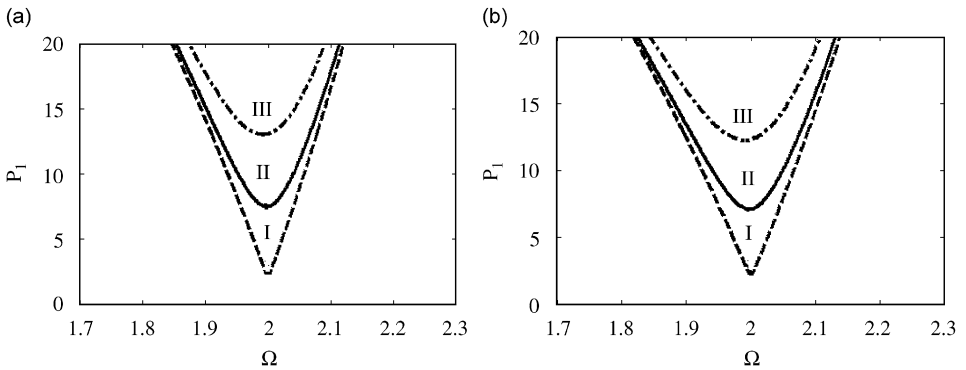

Fig. 12. Influence of the mass ratio in periodic axial force on the transition curves for $P_0 = 1.0$ and $B_m = 0.3$, (I) $C_d = 0.0$, (II) $C_d = 0.2$ and (III) $C_d = 0.4$; (a) $\bar{m} = 0.1$ and (b) $\bar{m} = 0.2$.

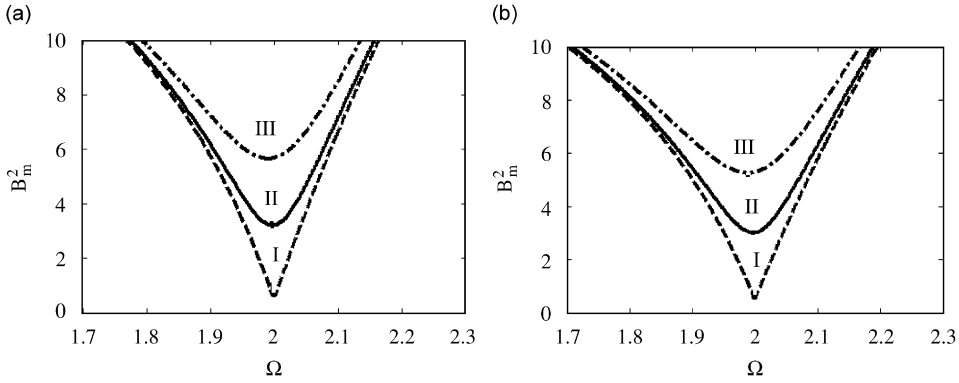

Fig. 13. Influence of the mass ratio in magnetic field on the transition curves for $P_1 = 1.0$ and $P_0 = 1.0$, (I) $C_d = 0.0$, (II) $C_d = 0.2$ and (III) $C_d = 0.4$; (a) $\bar{m} = 0.1$ and (b) $\bar{m} = 0.2$.

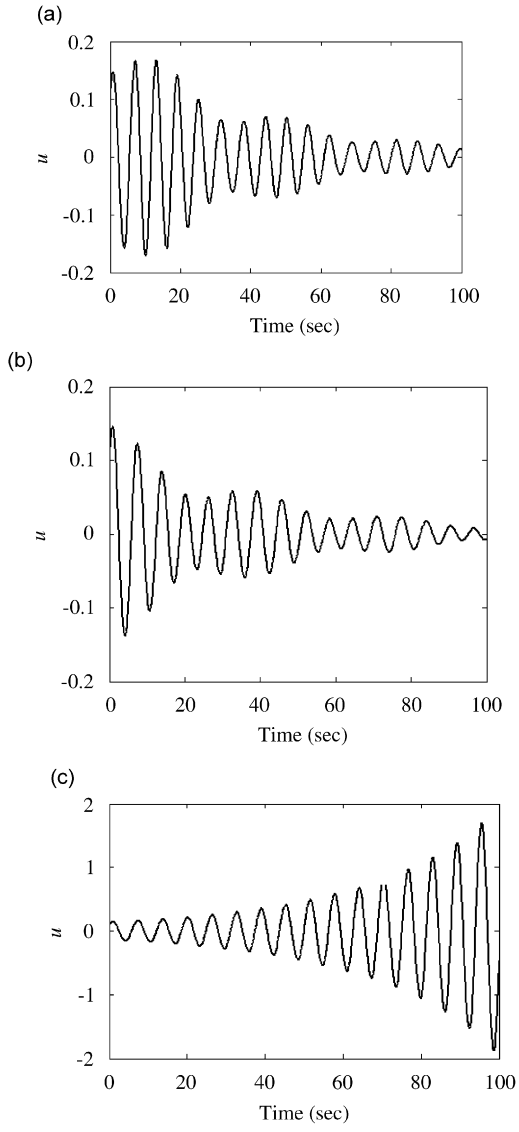

Fig. 14. Time response for (a) point C; (b) point B and (c) point A; key as in Fig. 10(a, II).

system improves. One may find a critical value P_1 below which the system is always stable. For example, from Fig. 10(b) for the system with $C_d = 0.2$ the critical value P_1 is 5.05. These values will be very much useful for designing the flexible manipulators.

The influence of static load P_0 on the instability regions $B_m^2 \sim \Omega$ is shown in Figs. 11(a and b) and it is observed that with increase in P_0, the instability region decreases. For example, from Fig. 11(a, III) the system is always stable for a magnetic field of B_m^2 less than 3.1 and with increase of P_0 to 5 this critical value of B_m^2 increases to 3.95.

Figs. 12 and 13 show the influence of mass ratio $\bar{m}$ on the parametric instability regions in $P_1 \sim \Omega$ and $B_m^2 \sim \Omega$ plane, respectively. One may observe that similar to the previous cases, here also with increase in $\bar{m}$ the region of instability increases.

Similar to previous cases, here the results from the perturbation analysis are compared by plotting the time response, which are obtained by numerically solving the temporal equation of motion (Eq. (7)). Figs. 14(a–c) correspond respectively to the points A, B and C of Fig. 10(a, II). They are found to be in good agreement.

5. Conclusions

In this work, the stability boundaries of a cantilever beam with and without tip mass subjected to time-varying transverse magnetic field and axial periodic load are studied. The nonlinear temporal equation of motion, which contains two frequency parametric excitation terms, is solved using second-order method of multiple scales. Instability regions are found for three different resonance conditions viz., simple resonance, principal parametric resonance and simultaneous principal parametric and simple resonance. In case of simple resonance, the instability region is compared with the experimental work and is found to be in good agreement.

One may use Eqs. (29)–(31) to determine the parametric instability regions for different resonance conditions for any similar physical system. In all the cases, it is observed that with increase in damping and static axial load or decrease in mass ratio the instability region decreases and one may control the vibration of a system using required magnetic field as shown in the figures with parametric instability regions.

Acknowledgment

The authors thank Professor G.Y. Wu who provided his manuscript [4] that is used for comparison purpose in this work.

References

[1] F.C. Moon, Y.H. Pao, Vibration and dynamic instability of a beam-plate in a transverse magnetic field, *Journal of Applied Mechanics* 36 (1969) 92–100.
[2] H. Kojima, K. Nagaya, Nonlinear forced vibration of a beam with a mass subjected to alternating electromagnetic force, *Bulletin of the Japan Society of Mechanical Engineers* 28 (1985) 468–474.
[3] Q.S. Lu, C.W.S. To, K.L. Huang, Dynamic stability and bifurcation of an alternating load and magnetic field excited magneto-elastic beam, *Journal of Sound and Vibration* 181 (1995) 873–891.
[4] G.Y. Wu, R. Tsai, Y.S. Shih, The analysis of dynamic stability and vibration motions of a cantilever beam with axial loads and transverse magnetic fields, *Journal of the Acoustical Society of ROC* 4 (1997) 40–55.
[5] Y.S. Shih, G.Y. Wu, J.S. Chen, Transient vibrations of a simply supported beam with axial loads and transverse magnetic fields, *Mechanics of Structures and Machines* 26 (1998) 115–130.
[6] C.C. Chen, M.K. Yah, Parametric instability of a beam under electromagnetic excitation, *Journal of Sound and Vibration* 240 (2001) 747–764.
[7] G.Y. Wu, The analysis of dynamic instability and vibration motions of a pinned beam with transverse magnetic fields and thermal loads, *Journal of Sound and Vibration* 284 (2005) 343–360.
[8] M.F. Liu, T.P. Chang, Vibration analysis of a magneto-elastic beam with general boundary conditions subjected to axial load and external force, *Journal of Sound and Vibration* 288 (2005) 399–411.
[9] S.Z.H. Burney, L.G. Jager, A method of determining the regions of instability of a column by a numerical approach, *Journal of Sound and Vibration* 15 (1971) 75–91.
[10] R.C. Kar, T. Sujata, Parametric instability of an elastically restrained cantilever beam, *Computers and Structures* 34 (1990) 469–475.

[11] C.C. Chen, M.K. Yah, Parametric instability of a column with axially oscillating mass, *Journal of Sound and Vibration* 224 (1999) 643–664.
[12] H. Hyun, H.H. Yoo, Dynamic modeling and stability analysis of axially oscillating cantilever beams, *Journal of Sound and Vibration* 228 (1999) 543–558.
[13] J. Chung, D. Jung, H.H. Yoo, Stability analysis for the flap wise motions of cantilever beam with rotary oscillation, *Journal of Sound and Vibration* 273 (2004) 1047–1062.
[14] A.H. Nayfeh, D.T. Mook, *Nonlinear Oscillations*, Wiley, New York, 1995.
[15] A.H. Nayfeh, B. Balachandran, *Applied Nonlinear Dynamics—Analytical, Computational and Experimental Methods*, Wiley, Canada, 1995.